A New Way of Analyzing Vibrational Spectra. IV. Application and Testing of Adiabatic Modes Within the Concept of the Characterization of Normal Modes

ZORAN KONKOLI, J. ANDREAS LARSSON, DIETER CREMER

Department of Theoretical Chemistry, University of Göteborg, Kemigården 3, S-41296 Göteborg, Sweden

Received 24 March 1997; revised 30 September 1997; accepted 8 October 1997

ABSTRACT: The CNM (characterization of normal modes) method for extracting chemical information out of vibrational spectra is tested for vibrational spectra of molecules with relatively strong or relatively weak coupling between internal vibrational modes. Symmetry, parameter set stability, and frequency uncertainty tests are applied to check whether internal vibrational modes, internal mode frequencies, and amplitudes $\mathscr{A}_{n\mu}$ comply with symmetry, are independent of the set of internal parameters ζ_n used to describe molecular geometry or fulfill a Lorentzian correlation between amplitudes $\mathscr{A}_{n\mu}$ and frequency differences $\Delta\omega_{n\mu} = \omega_n - \omega_\mu$. In all cases considered, amplitudes $\mathscr{A}_{n\mu}$ based on adiabatic internal modes and mass or force constant matrices as metric **O** are superior to any other definition of amplitude. They represent the basic elements of the new CNM method that leads to chemically reasonable results and presents a new way of extracting chemical information out of vibrational spectra. A number of deficiencies of the potential energy distribution (PED) analysis is discussed. Int J Quant Chem **67**: 41–55, 1998

Introduction

In article III [1] of this series [2, 3], we outlined the concept of characterizing normal modes (CNM) $\mathbf{l}_\mu$ obtained in the course of the normal mode analysis (NMA) of vibrational spectroscopy [4–7]. Essential for the CNM concept is the comparison of the delocalized normal modes $\mathbf{l}_\mu$ of a molecule with the localized internal modes $\mathbf{v}_n$ of its fragments and structural units ϕ_n. With the help of NMA, which leads to the normal modes $\mathbf{l}_\mu$, and CNM, that extracts chemically important information out of the normal vibrational modes $\mathbf{l}_\mu$ utilizing internal modes $\mathbf{v}_n$, any molecule can be systematically investigated with regard to bonding characteristics, bond angle strain, conformational flexibility, torsional strain (using internal modes

Correspondence to: D. Cremer.

Contract grant sponsor: Swedish Natural Science Research Council (NFR).

CCC 0020-7608 / 98 / 010041-15

associated with torsional angles), etc. In this way, the complete information embedded in vibrational spectra can be extracted to add to the understanding of molecular geometry and conformation, electronic structure, and stability as well as other properties that can be associated with certain structural units of the molecule.

The prerequisite of the CNM approach is the definition and determination of appropriate internal vibrational modes associated with the internal parameters ζ_n (e.g., internal coordinates q_n) of a molecule. The CNM methods best known are the potential energy distribution (PED) analysis [8–10] and its recent extension suggested by Boatz and Gordon (BG approach) [11]. In article II [3] of this series, we showed that both methods are based on the vectors $\mathbf{c}_n$ (''**c**-vectors'') of Neto's **C**-matrix that transforms internal coordinates q_n into Cartesian coordinates $\mathbf{x}_i$ [12]. We also showed on theoretical grounds that **c**-vectors have a number of disadvantages, but so far it is not clear whether these disadvantages will really be of importance in applications such as the PED analysis. The present article was aimed at clarifying this question.

The second prerequisite of a useful CNM analysis is the definition of an appropriate tool to compare normal vibrational modes and internal vibrational modes. In article III [1], we discussed various definitions of an appropriate amplitude $\mathscr{A}_{n\mu}$ that relates an internal mode $\mathbf{v}_n$ to a normal mode $\mathbf{l}_\mu$. A priori, there are no strict physical rules that help to define amplitude $\mathscr{A}_{n\mu}$. However, we showed that $\mathscr{A}_{n\mu}$ should fulfill three criteria: (1) Symmetry equivalent amplitudes have to adopt the same value (*symmetry criterion*). (2) The value of $\mathscr{A}_{n\mu}$ should be stable with regard to variations in the set of internal parameters used: $\Delta\mathscr{A}_{n\mu} = |\mathscr{A}_{n\mu}(\mathrm{PSA}) - \mathscr{A}_{n\mu}(\mathrm{PSB})| = 0$ (PS: parameter set) for any ζ_n* used in both PSA and PSB (*parameter set stability criterion*). (3) The distribution of amplitude values $\mathscr{A}_{n\mu}$ in dependence of the frequency difference $\Delta\omega_{n\mu} = \omega_n - \omega_\mu$ should be enveloped by a Lorentzian (bell-shaped) curve since small differences $\Delta\omega_{n\mu}$ can lead to large (or in exceptions to small) $\mathscr{A}_{n\mu}$ values while large differences $\Delta\omega_{n\mu}$ should always lead to small $\mathscr{A}_{n\mu}$ values. This implies that the product $h_{n\mu} = \mathscr{A}_{n\mu}\Delta\omega_{n\mu}$ never exceeds a certain (relatively small) limit value (*frequency uncertainty criterion*) [1].

* We use internal parameters ζ_n rather than internal coordinates q_n since the former cover all possible choices of a coordinate (puckering coordinates [13a], natural coordinates [13b], delocalized coordinates, etc.).

Considering the two available definitions of internal modes $\mathbf{v}_n$($\mathbf{a}_n$ and $\mathbf{c}_n$) as well as the various possibilities of defining an amplitude, 12 different ways of defining a suitable amplitude for use in the CNM analysis were discussed in article III [1]. On purely theoretical grounds, it was shown that the most useful amplitudes A should be those which compare an adiabatic internal mode vector $\mathbf{a}_n$ and a normal mode vector $\mathbf{l}_\mu$ either kinetically [''mass comparison,'' Eq. (1)] or dynamically [''force comparison'', Eq. (2)] since they show the influence of $\mathbf{a}_n$ on the form of the normal mode vector $\mathbf{l}_\mu$ as transmitted via the distribution of atomic masses (by mass matrix **M**) or via the electronic structure (by force constant matrix **f**). These amplitudes are abbreviated as AvAM and AvAF:

$$AvAM = A_{n\mu}^{(M)} = \frac{(\mathbf{l}_\mu^+\mathbf{M}\mathbf{a}_n)^2}{(\mathbf{a}_n^+\mathbf{M}\mathbf{a}_n)(\mathbf{l}_\mu^+\mathbf{M}\mathbf{l}_\mu)} \qquad (1)$$

$$AvAF = A_{n\mu}^{(F)} = \frac{(\mathbf{l}_\mu^+\mathbf{f}\mathbf{a}_n)^2}{(\mathbf{a}_n^+\mathbf{f}\mathbf{a}_n)(\mathbf{l}_\mu^+\mathbf{f}\mathbf{l}_\mu)} \qquad (2)$$

as was explained in article III [1].

Although the theoretical analysis gives convincing arguments to apply the amplitudes of Eqs. (3) and (4) rather than one of the possible alternative definitions, it is not clear whether the deficiencies of *P*-type amplitudes or *c*-vector-based amplitudes really matter in practical considerations. Almost all CNM-related work of the last 30 years has been carried out with the PED analysis and obvious deficiencies such as negative or exceedingly large amplitude values have simply been regarded as not changing the chemical information of the PED analysis. Therefore, it has to be clarified in this work whether the theoretical advantages of the use of the adiabatic internal mode vectors in connection with the amplitudes of Eqs. (1) and (2) pays out in practice and leads to a CNM method that is clearly superior to the PED analysis and its extensions.

We proceed in this work by applying the CNM analysis to calculated vibrational spectra of a number of nontrivial molecules. Primarily, the symmetry criterion, PS stability, and the frequency uncertainty criterion will be used to determine reliability and chemical usefulness of the results of the CNM analysis when using different internal modes, different definitions of an amplitude, different metrics for the comparison, and different

definitions of the internal mode frequency. The outcome of this investigation will lead to a theoretically as well as practically tested new CNM method.

Computational Methods

Molecules **1**–**9** investigated in this work are shown in Figure 1. Hartree–Fock (HF) theory in connection with the 6-31G(d, p) basis set [14] was used to calculate equilibrium geometries and harmonic vibrational frequencies. These data together with all internal vibrational frequencies calculated in this work (27 tables) are available from the authors.

A complete set of internal parameters [11] to carry out the CNM analysis for the $3K - L$ normal modes of a molecule requires $3K - L$ coordinates associated with $3K - L$ structural units. In case of symmetry, some of the $3K - L$ internal modes have to be symmetry equivalent and this provides an additional test for the applicability of internal mode vectors and the amplitude used. We note that in the case of adiabatic mode vectors that a complete parameter set is not needed; however, to generate in one calculation also those internal modes and internal mode frequencies that require complete parameter sets, throughout this work, sets of $3K - L$ internal coordinates are used. These sets are denoted as nonredundant parameter sets PS, while redundant PS are indicated by RPS.

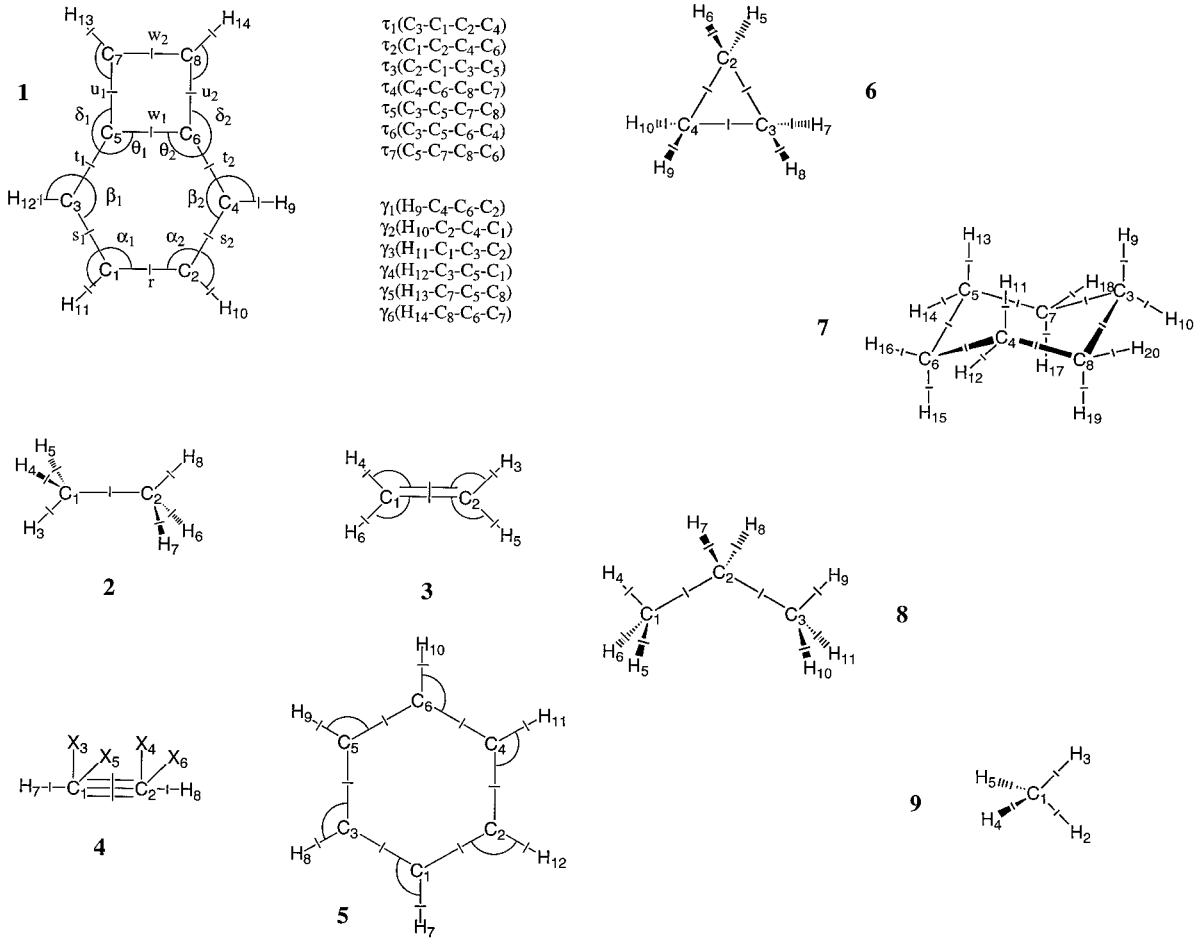

FIGURE 1. Molecules **1–9** investigated in this work. Numbering of atoms and notations for some internal coordinates q_n are given. Bond lengths included into the PS are indicated by a perpendicular line through the bond, and bond angles by an arc connecting relevant bonds. Torsional angles τ and out-of-plane bending angels γ are given for molecule **1**. In the case of ethyne (**4**), dummy atoms needed for the definition of bending angles are denotes as X. For a more detailed description of PSs, see Table I.

TABLE I

Parameter sets (PS) used in the CNM analysis of molecules 1–9.

No.	Molecule	Sym	PS	R / N[a]	Parameters	N[b]
1	Benzo-cyclobutadiene	C_{2v}	PS0	—	All CH bonds, 6 of 12 CCH angles, $\tau_1-\tau_5$, $\gamma_1-\gamma_6$	23
			PS1	N	PS0 U $\{r, s_1, s_2, t_1, t_2, u_1, u_2, \alpha_1, \alpha_2, \beta_1, \beta_2, \delta_1, \delta_2\}$	36
			RPS2	R	PSO U $\{r, s_1, s_2, t_1, t_2, u_1, u_2, w_1, w_2, \alpha_1, \alpha_2, \beta_1, \beta_2, \delta_1, \delta_2\}$	38
			RPS3	R	PSO U $\{r, s_1, s_2, t_1, t_2, u_1, u_2, w_1, w_2, \alpha_1, \alpha_2, \beta_1, \beta_2, \theta_1, \theta_2, \delta_1, \delta_2\}$	40
			PS4	N	PSO U $\{r, s_1, s_2, t_1, t_2, u_1, u_2, \alpha_1, \alpha_2, \theta_1, \theta_2, \delta_1, \delta_2\}$	36
			RPS5	R	PSO U $\{r, s_1, s_2, t_1, t_2, u_1, u_2, w_1, w_2, \alpha_1, \alpha_2, \beta_1, \beta_2, \theta_1, \theta_2, \delta_1, \delta_2, \tau_6, \tau_7\}$	42
			PS6	N	PSO U $\{r, s_1, s_2, t_1, t_2, u_1, u_2, w_1, \alpha_1, \alpha_2, \beta_2, \delta_1, \delta_2\}$	36
			RPS7	R	PSO U $\{s_1, s_2, t_1, t_2, u_1, u_2, w_1, w_2, \alpha_1, \alpha_2, \beta_1, \beta_2, \theta_1, \theta_2, \delta_1, \delta_2\}$	39
			PS8	N	PSO U $\{r, s_1, s_2, t_1, t_2, u_1, u_2, w_1, w_2, \alpha_1, \alpha_2, \beta_2, \delta_1\}$	36
			PS9	N	PSO U $\{s_1, s_2, t_1, t_2, u_1, u_2, w_1, \alpha_1, \alpha_2, \beta_1, \beta_2, \delta_1, \delta_2)$	36
2	Ethane	D_{3d}	PS1	N	CC, all CH, all CCH, $H_3C_1H_4$, $H_4C_1H_5$, $H_6C_2H_7$, $H_6C_2H_8$, $\tau(H_3C_1C_2H_6)$	18
3	Ethene	D_{2h}	PS1	N	CC, all CH, all CCH, $\tau(H_4C_1C_2H_3)$, $\tau(H_6C_1C_2H_5)$, $\tau(H_4C_1C_2H_5)$	12
4	Ethyne	$D_{\infty h}$	PS1	N	CC, all CH, $\tau(H_7C_1X_3C_2)$, $\tau(H_7C_1X_5C_2)$, $\tau(H_8C_2X_4C_1)$, $\tau(H_8C_2X_6C_1)$	7
5	Benzene	D_{6h}	PS0	—	All CC, all CH, 6 of the 12 CCH, $\gamma_1-\gamma_6$	24
			PS1	N	PSO U $(C_2C_1C_3, C_2C_4C_6, C_3C_5C_6, \tau(C_4C_2C_1C_3), \tau(C_6C_5C_3C_1), \tau(C_5C_6C_4C_2)$	30
			PS2	N	PSO U $\{C_2C_1C_3, C_2C_4C_6, C_1C_2C_4, \tau(C_4C_2C_1C_3), \tau(C_6C_5C_3C_1), \tau(C_5C_6C_4C_2)$	30
6	Cyclopropane	D_{3h}	PS1	N	All CC, all CH, all CCH	21
7	Cyclohexane	D_{3d}	PS1	N	All CC, all CH, all CCC, all CCH	48
8	Propane	D_{2v}	PS1	N	all CC, all CH, CCC, all CCH, $H_4C_1H_5$, $H_4C_1H_6$, $H_9C_3H_{10}$, $H_9C_3H_{11}$, $\tau(H_4C_1C_2C_3)$, $\tau(H_9C_3C_2C_1)$	27
9	Methane	T_d	PS1	N	All CH, $H_2C_1H_3$, $H_3C_1H_4$, $H_4C_1H_5$, $H_5C_1H_2$, $H_2C_1H_4$	9

[a] R / N denotes a redundant or nonredundant PS.

[b] Number of parameters for a complete PS.

In Table I, the PSs for molecules **1**–**9** are given. In some cases, different PSn for one molecule were tested, which are also listed in Table I (compare with Fig. 1 for the numbering of atoms). In particular, it was tested how the CNM analysis is influenced by using RPS with more than $3K - L$ internal coordinates. The internal coordinates included into a PS comprise bond lengths $r(AB)$, bond angles $\alpha(ABC)$, torsion angles $\tau(ABCD)$, and out-of-plane angles $\gamma(ABCD)$, where γ describes the bending of bond AB out of the plan BCD.

The examples chosen in this work cover acyclic molecules with a modest coupling between internal vibrational modes and cyclic or bicyclic molecules with considerable coupling between internal modes. Also, molecules of high and relatively low symmetry are considered. The number of molecules investigated is actually much larger than that shown in Figure 1; however, we refrain from presenting all data here, since for a critical discussion of the CNM method and the amplitudes suggested in article III [1], a selected data set represented by molecules **1**–**9** is sufficient.

In each case, internal mode frequencies ω_n associated with adiabatic mode vectors $\mathbf{a}_n$ (denoted as ω_a), the intrinsic frequencies of Boatz and Gordon (denoted as ω_{BG} or $\omega_{n,BG}$) [11], which are based on **c**-vectors (or, alternatively, on **a**-vectors [2]), and the internal mode frequencies associated with **c**-vectors (denoted as ω_c) are calculated together with the 12 different amplitudes $\mathscr{A}_{n\mu}$ described in article III [1] and denoted in the following way:

1. AvAS: Amplitudes $A_{n\mu}$ based on **a**-vectors using the overlap matrix $\mathbf{S} = \mathbf{I}$ as a metric.
2. AvPS: Amplitudes P_{nn}^{μ} based on **a**-vectors using the overlap matrix $\mathbf{S} = \mathbf{I}$ as a metric.
3. CvAS: Amplitudes $A_{n\mu}$ based on **c**-vectors using the overlap matrix $\mathbf{S} = \mathbf{I}$ as a metric.
4. CvPS: Amplitudes P_{nn}^{μ} based on **c**-vectors using the overlap matrix $\mathbf{S} = \mathbf{I}$ as a metric.
5. AvAM: Amplitudes $A_{n\mu}$ based on **a**-vectors using the mass matrix **M** as a metric.
6. AvPM: Amplitudes P_{nn}^{μ} based on **a**-vectors using the mass matrix **M** as a metric.
7. CvAM: Amplitudes $A_{n\mu}$ based on **c**-vectors using the mass matrix **M** as a metric.
8. CvPM: Amplitudes P_{nn}^{μ} based on **c**-vectors using the mass matrix **M** as a metric.
9. AvAF: Amplitudes $A_{n\mu}$ based on **a**-vectors using the force constant matrix **f** as a metric.
10. AvPF: Amplitudes P_{nn}^{μ} based on **a**-vectors using the force constant matrix **f** as a metric.
11. CvAF: Amplitudes $A_{n\mu}$ based on **c**-vectors using the force constant matrix **f** as a metric.
12. CvPF: Amplitudes P_{nn}^{μ} based on **c**-vectors using the force constant matrix **f** as a metric.

Absolute amplitudes $\mathscr{A}$ and normalized amplitudes $\mathscr{A}^{\%}$ are considered in the following where the latter used for a comparison of A-type and P-type amplitudes. In this connection, we have to note that due to normalization amplitudes are no longer independent of the parameter set chosen. Calculations have to show whether this effect is negligible or contaminates the results of the CNM analysis.

Results and Discussion

The simplest test that can be carried out to investigate the usefulness of a given definition of amplitude is provided by a symmetry test.

SYMMETRY PROBLEM OF c-VECTORS

Due to the strong PS dependence of **c**-vectors [3], it can happen that a complete (nonredundant) PS [11] leads to nonsymmetric **c**-vectors. In Figure 2, absolute CvAF and CvPF amplitudes are given for the six internal CC stretching motions of the planar benzene ring which is defined by $2K - 3 = 9$ internal parameters (K: number of atoms). PS2 is used (Table I), in which the carbon framework of benzene is described by six C—C bond lengths and three CCC bond angles (see Fig. 2). For the symmetric breathing mode, the six symmetry-equivalent internal CC stretching modes adopt different amplitudes as a result of the fact that the six **c**-vectors representing CC stretching *are not symmetry-equivalent*. Both absolute CvAF and CvPF amplitudes do not fulfill the D_{6h} symmetry of benzene and even C_2 symmetry (with C_1C_6 being the C2 axis) is slightly broken because of a nonsymmetric choice of the CCH bending angles (Fig. 2). Clearly, the symmetry problem of the **c**-vectors makes both the PED analysis (CvPF) and the use of A amplitudes (CvAF) worthless.

Of course, in the case of benzene, the symmetry problem can easily be solved by including three redundant CCC bending angles. However, in case of nonsymmetric molecules, there are no symmetry criteria that help to choose a proper set of

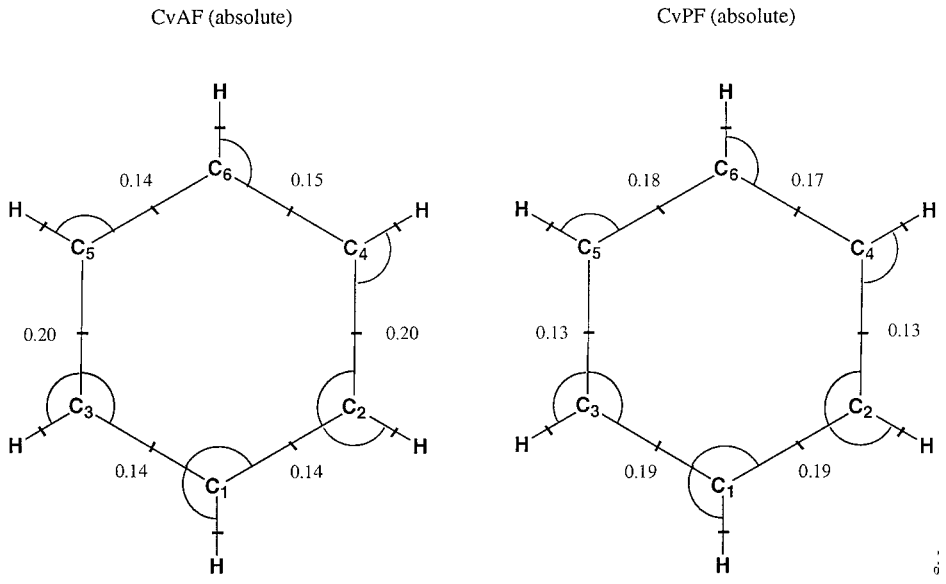

FIGURE 2. Absolute amplitudes CvAF and CvPF of the six CC stretching modes calculated at HF / 6-31G(*d*, *p*) for the normal mode that corresponds to symmetric breathing of the benzene (**5**) ring. Benzene is described by parameter set PS2.

internal parameters. Clearly, **c**-vectors suffer from the symmetry problem and, therefore, are not suitable for use in the CNM analysis.

PS STABILITY TEST OF AMPLITUDES

This test will be discussed for benzocyclobutadiene (**1**), which due to its planarity is easy to interpret; however, due to its bicyclic nature, it does not offer any guidance for setting up the most reasonable complete PS. In Table I, nine nonredundant or redundant PSs of **1** are listed. For all nine PSs, normal mode frequencies, internal mode frequencies, and amplitudes are calculated, where the latter are compared for two different PSs (see Article III [1]). In Figure 3, four possible combinations of PSs are considered, namely, pair PSP1 corresponding to the combination of RPS2 and RPS3, PSP2 to RPS3 and RPS7, PSP3 to PS1 and PS9, and PSP4 to PS1 and PS4. These combinations describe the situation of adding two redundant parameters to an RPS (PSP1, the internal ring angles θ_1 and θ_2 are added), of deleting the ring bond length r in an RPS (PSP2), of replacing r by the bond length w_1 in a nonredundant PS (PSP3), and of replacing two internal ring angles (β_1, β_2) by two others in a nonredundant PS (PSP4). None of these PS changes can be considered as leading to a better or worse description of **1** in a chemical or geometrical sense. We tested also other combinations, which yielded much more serious changes, e.g., when breaking the C_{2v} symmetry of **1** by deleting one of two symmetry-equivalent parameters. Hence, the changes described by pairs PSP1 to PSP4 can be considered to be so smooth that they should not affect calculated amplitudes significantly.

In Figure 3, for each pair of PSs, a bar diagram of calculated $\Delta\mathscr{A}_{n\mu}$ values vs. common internal coordinates q_n is show for absolute CvAF amplitudes. Points with $\Delta\mathscr{A}_{n\mu} = 0$ were removed to condense the presentation. Figure 3 reveals relatively large instabilities of CvAF amplitudes up to 0.5, which is considerable in view of the fact that all normal modes in **1** are strongly delocalized and none of them is associated with a large amplitude. Clearly, these amplitudes are rather unstable, which originates from the instability of **c**-vectors with regard to PS changes [1–3].

In Figures 4(a)–4(d), the four amplitudes AvAF, AvPF, CvAF, and CvPF in their normalized form are compared, again using **1** as an appropriate, nontrivial test example and considering PS pairs PSP1{RPS2, RPS3}, PSP2{RPS3, RPS7}, PSP3{RPS2, PS8}, PSP4{PS1, PS9} (= PSP3 in Figure 3), PSP5{PS1, PS4} (= PSP4 in Figure 3), and PSP6{PS1, PS6}, thus adding to the four combinations considered in Figure 3 also two pairs, which

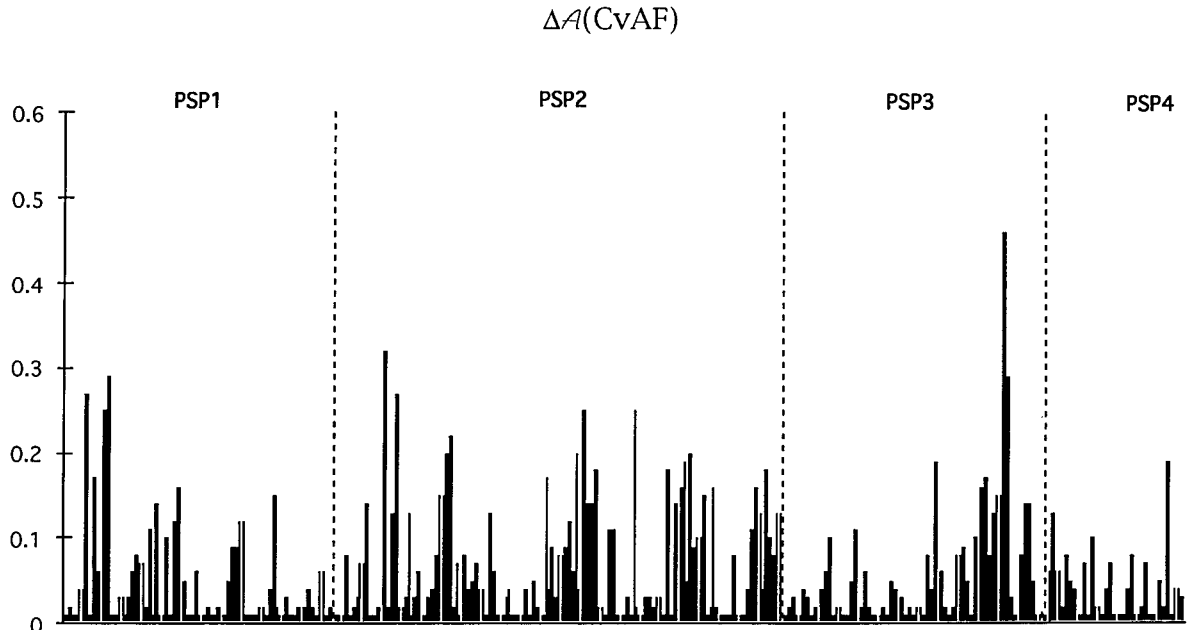

FIGURE 3. PS instability test of **c**-vectors in the case of benzocyclobutadiene (**1**) [HF / 6-31G(*d*, *p*) calculations]. The four pairs of parameter sets PSP1{RPS2, RPS3}, PSP2{RPS3, RPS7}, PSP3{PS1, PS9}, and PSP4{PS1, PS4} correspond to systematic variations in the PS as described in the text. The difference $\Delta\mathscr{A}$ in absolute CvAF amplitudes is plotted for each PSP vs. the internal parameters $\zeta_n = q_n$ common to both sets. Points corresponding to $\Delta\mathscr{A} = 0$ have been removed. Vertical dashed lines indicate borders between different parameter set pairs.

describe changes from symmetrical to nonsymmetrical PS (PSP3 and PSP6).

Apart from deleting all points in the diagrams of Figure 4, for which

$$0 = \Delta\mathscr{A}_{n\mu}(\text{AvAF}) = \Delta\mathscr{A}_{n\mu}(\text{AvPF}) = \Delta\mathscr{A}_{n\mu}(\text{CvAF}) = \Delta\mathscr{A}_{n\mu}(\text{CvPF}),$$

since they are not relevant for the PS stability test, only those normal modes were considered, for which the amplitudes of internal modes being excluded (PSP1−3) or replaced (PSP4−6) are smaller or equal to 1%. In this way, a flow of percentage from or to the common set of internal parameters within PSPn is avoided. Hence, the differences $\Delta\mathscr{A}$ shown in Figure 4 solely originate from a fluctuation of amplitudes for those internal modes that are associated with internal parameters common to PSP and, therefore, the results of Figure 4 provide a reliable insight into the stability (instability) of $\mathscr{A}$ with regard to PS changes.

Figure 4(a) confirms that adiabatic internal mode vectors do not depend on the choice of the parameters set since $\Delta\mathscr{A}$ values are vanishing small for AvAF amplitudes. There are some small deviations from zero (less than 3%), which result from the fact that normalized amplitudes have to be used to compare *A*- and *P*-type amplitudes. Clearly, the PS dependence introduced in this way [1] is not that serious to refrain from using normalized amplitudes.

P-type amplitudes clearly suffer from PS instabilities even if the internal mode vectors are PS independent as in the case of AvPF amplitudes [see, e.g., PSP1 and PSP4−PSP6) in Fig. 4(b)], for which the maximum deviations are as large as 20%. This holds for both redundant parameter set pairs (PSP1, PSP2) and nonredundant parameter set pairs (PSP4−PSP6). The instability of *P*-type amplitudes results from the fact that they depend on the normal mode vectors $\mathbf{l}_\mu$, which, in turn, are expressed as linear combinations of internal modes vectors $\mathbf{v}_n$. Since the individual coefficients in the expansion can change drastically upon replacement of one or more of the basis vectors $\mathbf{v}_n$, *P*-type amplitudes will generally suffer from the PS-instability problem.

In Figure 3, it is shown that the instability of **c**-vectors can influence the instability of absolute CvAF amplitudes. This is confirmed for normal-

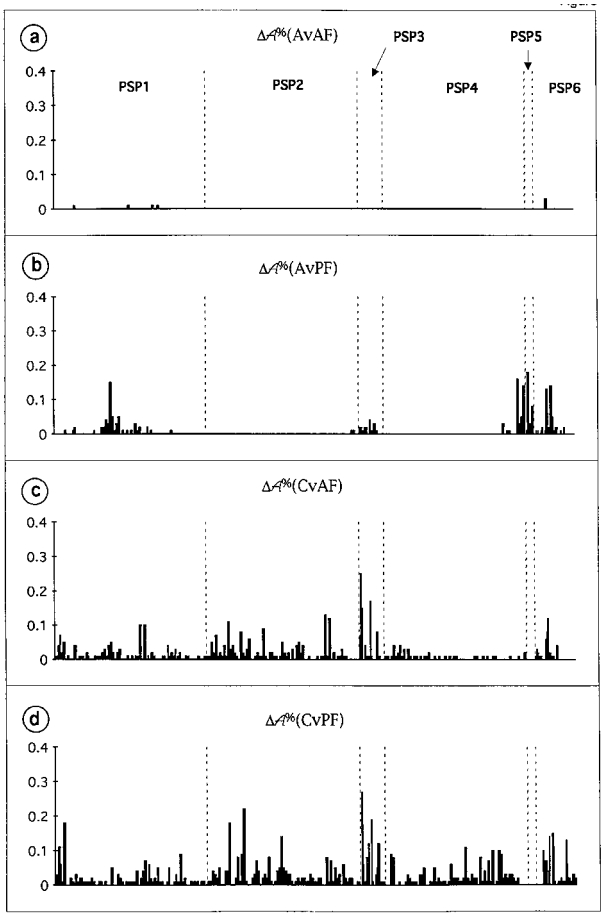

FIGURE 4. PS instability test for *A*- and *P*-type amplitudes in the case of benzocyclobutadiene (**1**) [HF / 6-31G(*d*, *p*) calculations]. Amplitues (a) AvAF, (b) AvPF, (c) CvAF, and (d) CvPF and parameter set pairs PSP1{RPS2, RPS3}, PSP2{RPS3, RPS7}, PSP3{RPS2, PS8}, PSP4{PS1, PS9}, PSP5{PS1, PS4}, and PSP6{PS1, PS6} were considered. Amplitudes are normalized to make a comparison between *P*-type and *A*-type amplitudes possible. The differences $\Delta\mathscr{A}^{\%}$ are plotted for each PSP vs. the internal parameters $\zeta_n = q_n$ common to both sets in a PSP. Points corresponding to $\Delta\mathscr{A} = 0$ were removed. Vertical dashed lines indicate borders between different parameter set pairs.

ized CvAF amplitudes [Fig. 4(c)]. One can observe that the PS-instability problems increase from AvAF [Fig. 4(a)] to CvAF [Fig. 4(c)] and CvPF amplitudes [Fig. 4(d)], where in the latter case, problems arise from both the PS instability of **c**-vectors and that of *P*-type amplitudes. It is noteworthy that *the PED analysis* [8–10], *which uses CvPF amplitudes, is based on the worst of the four possibilities*.

FREQUENCY UNCERTAINTY TEST

We have shown in article III [1] that the general correlation pattern between differences $\Delta\omega_{n\mu} = \omega_n - \omega_\mu$ and amplitudes $\mathscr{A}_{n\mu}$ should be enveloped by a Lorentzian (bell-shaped) curve. This more qualitatively oriented analysis is carried out in Figure 5 for **1** using the nonredundant PS1 [Fig. 5(a)–(h)] and the strongly redundant RPS5 [Fig. 5(i)–5(l)] in connection with different amplitudes either based on adiabatic internal mode vectors $\mathbf{a}_n$ or **c**-vectors. In Figure 5(a)–(d), the characteristic fragment frequencies ω_n are defined according to Boatz and Gordon [11]. Figure 5(a)–5(d) can directly be compared with Figure 5(e)–(h), which give the situation for fragment frequencies ω_n associated with internal mode vectors $\mathbf{v}_n(\mathbf{v}_n = \mathbf{a}_n$ or $\mathbf{v}_n = \mathbf{c}_n)$ defined in article I [2].

There are no significant differences in the correlation patterns of the amplitudes in Figure 5(a)–(d). However, each correlation pattern deviates from a Lorentzian (bell-shaped) form. No matter what definition of $\mathscr{A}_{n\mu}$ is used, there are always a considerable number of $(\mathscr{A}_{n\mu}, \Delta\omega_{n\mu})$ points outside the ideal correlation area. In figure 5(e)–(h), there are relatively large differences between the correlation patterns for Av- and Cv-type amplitudes where the former lead to clearly better results. In view of an expected Lorentzian-shaped correlation pattern $\mathscr{A}_{n\mu} - \Delta\omega_{n\mu}$, the worst result is obtained in the case of the CvPF amplitudes of the PED analysis, which again indicates that the PED approach is a rather poor basis for carrying out a CNM investigation. Replacing the *P*-type amplitude by the corresponding *A*-type amplitude as in the CvAF diagram improves the situation somewhat; however, it still reveals severe shortcomings of the description, which is obviously a result of the shortcomings of the **c**-vectors [3].

Clearly, the best correlation pattern complying exactly with the expected Lorentzian form is obtained in the case of the AvAF amplitudes in connection with a comparison of frequencies ω_μ with adiabatic internal frequencies ω_a. Adiabatic internal modes, the amplitude definition worked out in article III [1] and the force constant matrix **f** as a suitable metric for comparison provide the right ingredients for a physically well-founded CNM analysis. These ingredients, however, will not help if the internal mode frequency is defined as intrinsic frequency according to Boatz and Gordon [11] as is revealed by Figure 5(a) (AvAF vs. $\omega_{BG} - \omega_\mu$). On the one hand, the intrinsic frequen-

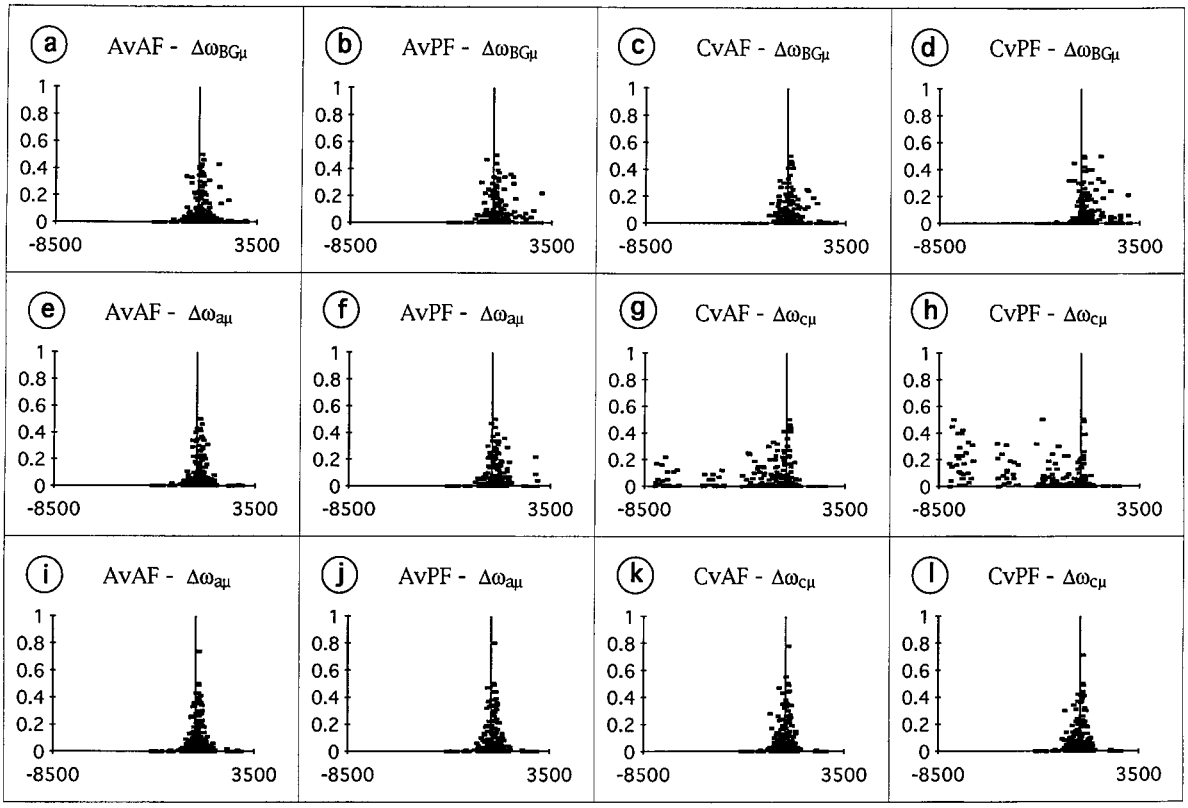

FIGURE 5. Frequency uncertainty test for benzocyclobutadiene (**1**) [HF / 6-31G(d, p) calculations]. Shown are the correlation diagrams between normalized amplitudes $A_{n\mu}$ and frequency differences $\Delta\omega_{n\mu} = \omega_n - \omega_\mu$, with ω_n being an internal mode frequency of a molecular fragment ϕ_n and ω_μ being a normal mode frequency. Amplitues AvAF, AvPF, CvAF, and CvPF are employed in connection with (a–d) intrinsic frequencies ω_{BG}, (e, f, i, j) adiabatic internal frequencies ω_a or (g, h, k, l) **c**-vector frequencies ω_c, using parameter set PS1 (a–h) or set RPS5 (i–l). In all cases, points that have $\Delta\mathscr{A} = 0$ for all tests within a given row of diagrams are removed.

cies do not reflect the advantages of AvAF amplitudes since they are insensitive to the deficiencies of **c**-vectors of P-type amplitudes. This is a consequence of defining intrinsic frequencies as averages over normal mode frequencies ω_μ, which makes them largely independent of the quality of both the internal mode vector $\mathbf{v}_n$ and the P-matrix elements.

Using a redundant PS as in the case of Figure 5(i)–(l), a significant improvement of all correlation patterns can be observed. This has to do with the fact that with increasing size of the redundant PS **c**-vectors adopt more the form of **a**-vectors. For example, in the case of the nonredundant PS1, the average overlap between adiabatic and **c**-vectors is 0.69, which means that the two type of internal mode vectors are indeed significantly different. In the case of the redundant PS5, the average overlap has increased to 0.84 without changing the form of the **a**-vectors from that of PS1 ($\mathbf{a}_n$ is completely PS independent), i.e., with increasing number of internal parameters, **c**-vectors will approach more and more the form of adiabatic vectors $\mathbf{a}_n$, which, accordingly, should be considered as the physically most reasonable ones.

The 12 diagrams of Figure 5 clearly demonstrate the superiority of adiabatic internal mode vectors in so far as they are PS independent and determined just by the electronic structure of the molecules investigated. Obviously, one can improve in critical cases the usefulness of **c**-vectors by using larger and larger redundant PS; however, this solution cannot be generalized, so that in specific cases, it will be difficult or even impossible to specify that RPS that guarantees the chemically most reliable CNM results.

QUANTIFICATION OF THE FREQUENCY UNCERTAINTY TEST BY USING $h_{n\mu}$

The $\mathscr{A}$-$\Delta\omega$ correlation diagrams provide a qualitative insight into the performance of particular amplitude $\mathscr{A}_{n\mu}$. A more quantitative insight is provided by the frequency uncertainty $h_{n\mu} = \mathscr{A}_{n\mu}\Delta\omega_{n\mu}$ given in cm^{-1} [1]. Amplitudes $\mathscr{A}_{n\mu}$ with a large value $h_{n\mu}$ are physically not reasonable while amplitudes $\mathscr{A}_{n\mu}$ with a low $h_{n\mu}$ value are reasonable. For example, if $\mathscr{A}_{n\mu} = 1$, then $h_{n\mu} = \Delta\omega_{n\mu}$ should be equal to zero since the normal mode $\mathbf{l}_\mu$ represents exclusively the internal motion $\mathbf{v}_n$ associated with the internal parameter $\zeta_n = q_n$, implying that $\omega_\mu = \omega_n$. If, however, $\omega_\mu \neq \omega_n$, i.e., $|\Delta\omega_{n\mu}| > 0$, then the error $h_{n\mu}$ will reveal right away deficiencies of the amplitude chosen to carry out the CNM analysis. All amplitudes $\mathscr{A}_{n\mu}$ with the same error $h_{n\mu}$ lie on the hyperbola $\mathscr{A}\Delta\omega = h$. For different h values, the curves with larger h are moved away from the origin.

In Figure 6, frequency uncertainty diagrams $h_{n\mu}$ corresponding to the $\mathscr{A}$-$\Delta\omega$ correlation diagrams of Figure 5 are shown. They prove a pointwise comparison of different amplitudes and, therefore, set a quantitative basis for the evaluation of different amplitudes. Averaged frequency uncertainties, $\bar{h}_{n\mu}$, calculated for the 12 cases of Figure 6 are listed in Table II. These data show that all the qualitatively formulated results of the analysis of the $\mathscr{A}$-$\Delta\omega$ correlation diagrams are confirmed by the frequency uncertainty diagrams and the average $h_{n\mu}$ values:

1. Adiabatic internal modes are clearly superior to **c**-vector modes as becomes obvious by

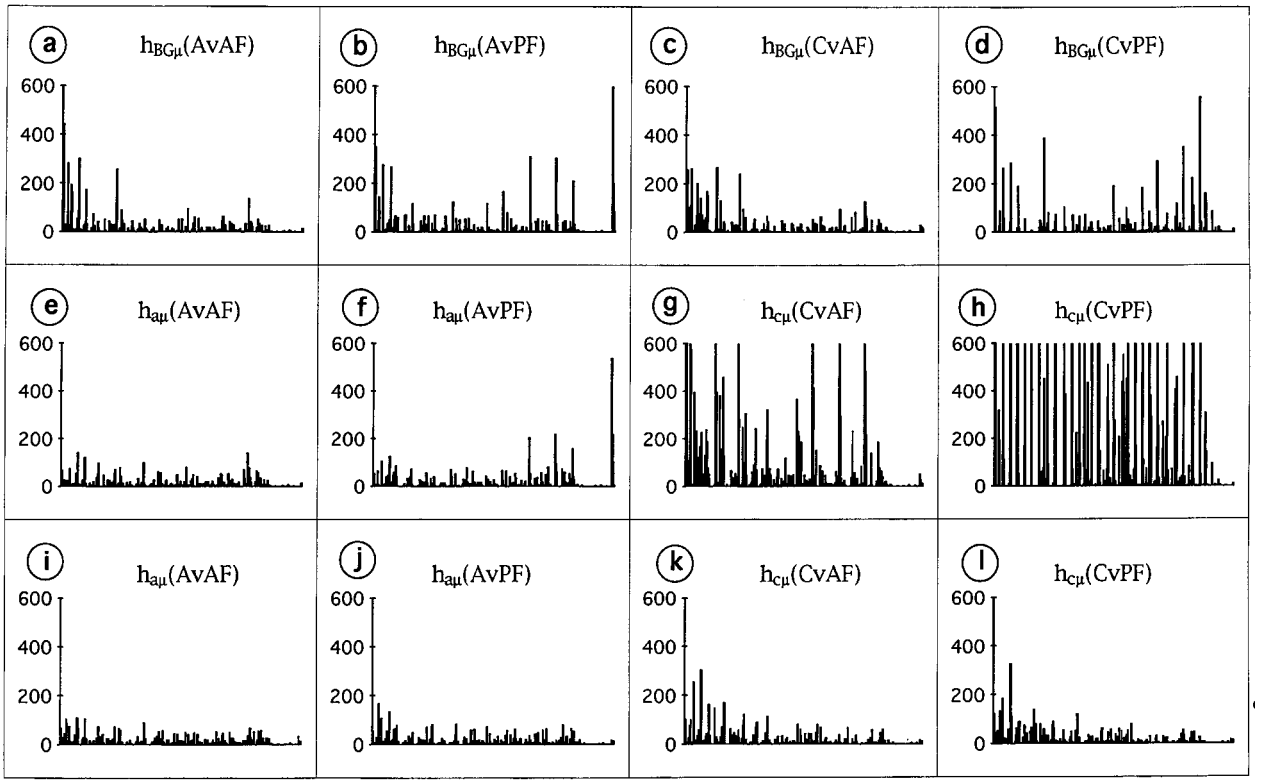

FIGURE 6. Frequency uncertainty test for benzycyclobutadiene (**1**) [HF / 6-31G(d, p) calculations]. The $h_{n\mu}$ diagrams corresponding to the tests of Figure 5 are shown. (a–d) Uncertainties $h_{n\mu}$ for amplitudes AvAF, AvPF, CvAF, and CvPF used in connection with intrinsic frequencies ω_{BG} (parameter set: PS1). (e–h) Uncertainties $h_{n\mu}$ for amplitudes AvAF, AvPF, CvAF, and CvPF used in connection with adiabatic internal frequencies ω_a and **c**-vector frequencies ω_c (parameter set: PS1) (i–l) Uncertainties $h_{n\mu}$ for amplitudes AvAF, AvPF, CvAF, and CvPF used in connection with adiabatic internal frequencies ω_a and **c**-vector frequencies ω_c (parameter set: RPS5). In all cases, $h_{n\mu}$ points that correspond to $\Delta\mathscr{A} = 0$ for all tests within a given row are removed. Large values of $h_{n\mu}$ were cut at 600 cm^{-1} to improve the representation.

TABLE II

Average frequency uncertainties $\bar{h}_{n\mu}$ calculated at HF / 6-31G(d, p) for benzocyclobutadiene (1) for different parameters sets (PS) (Table I), internal models $\mathbf{v}_n$, and internal frequencies according to the results summarized in Figure 6.[a]

PS	N / R	$\mathbf{v}_n$	ω_n	Amplitude $A_{n\mu}$	Uncertainty $\bar{h}_{n\mu}$	Increase in uncertainty	Figure
PS1	N	**a**	ω_{BG}	AvAF	16.3	0	6(a)
				AvPF	21.2	30.7	6(b)
		c		CvAF	17.7	8.8	6(c)
				CvPF	22.8	40.2	6(d)
PS1	N	**a**	ω_a	AvAF	12.0	0	6(e)
				AvPF	16.8	40.1	6(f)
		c		CvAF	67.3	461	6(g)
				CvPF	207.1	1726	6(h)
RPS5	R	**a**	ω_a	AvAF	10.9	0	6(i)
				AvPF	11.0	1.4	6(j)
		c		CvAF	14.2	30.5	6(k)
				CvPF	14.4	32.6	6(l)

[a] N and R denote nonredundant and redundant PS. The increase in uncertainty is given relative to AvAF values in %.

comparing $h_{n\mu}$ values in diagram 6(e) (AvAF) with those in diagram 6(g) (CvAF). Some of the h_c(CvAF) and h_c(CvPF) values are as large as 4000 cm^{-1}, which cannot be seen in Figure 6 since h values larger than 600 cm^{-1} have been cutoff for reasons of comparison.

2. Intrinsic frequencies [11] do not reflect the large difference between **a**- and **c**-vectors because of their average nature; however, in general, they lead to relatively large frequency uncertainties [Fig 6(a)–(d) and Table II].
3. *P*-type amplitudes always lead to larger uncertainties $h_{n\mu}$ than do *A*-type amplitudes (Table II; compare also Fig. 6(b) with (a), (d) with (c), (f) with (e), (h) with (g), etc.), which provides strong evidence for the deficiencies of the **P**-matrix approach as discussed in article III [1].
4. For redundant parameter sets such as RPS5, $h_{n\mu}$ values are considerably improved for **c**-vector-based amplitudes [Fig 6(k) and (l)] as well as *P*-type amplitudes [Fig 6(j) and (l)]; however, they do not reach the superior quality of AvAF amplitudes, which remains unaffected by any change in the PS [apart from normalization effects, compare Fig 6(e) and (i)].
5. The CvPF amplitudes of the PED analysis always lead to the largest frequency uncertainties and, therefore, should not be used.

We have used the $h_{n\mu}$ frequency uncertainty test to investigate amplitudes CvAF [Fig. 7(a)], CvPF [Fig. 7(b), AvAF [Fig. 7(c)], and AvPF [Fig. 7(d)] for molecules **2**–**9** always using a complete nonredundant PS as shown in Table I. Results of this investigation are summarized in condensed form in Figure 7 and Table III.

Contrary to the situation for molecule **1**, the difference between calculated $h_{n\mu}$ values in dependence of the choice of the amplitude seems to be smaller for molecules **2**–**9** (fig. 7). Averaged $h_{n\mu}$ values, $\bar{h}_{n\mu}$, range between 6 and 47 cm^{-1} (Table III), where the largest uncertainties are found for the CvPF amplitudes of the PED analysis. For comparing $\bar{h}_{n\mu}$ of molecules **2**–**9**, it is appropriate to define the average frequency uncertainty per normal mode $N\,\bar{h}_{n\mu} = \bar{h}_{\mu}$ also listed in Table III. Calculated values of $\bar{h}_{\mu}$ suggest that uncertainties increase with increasing coupling between internal modes, which is larger in cyclic rather than acyclic molecules. Hence, the largest $\bar{h}_{\mu}$ values are calculated for benzene, cyclohexane, and cyclopropane, while the smallest values are found for methane and ethane (results for AvAF, Table III). However, this ordering is lost for CvPF-related uncertainties, since in this case, all $\bar{h}_{\mu}$ values are relatively large. Nevertheless, the difference in uncertainties for AvAF and CvPF amplitudes are not so large for molecules **2**–**9** as in the case of **1**, which explains why the PED analysis was seemingly successful over decades. It simply has to do with the fact that

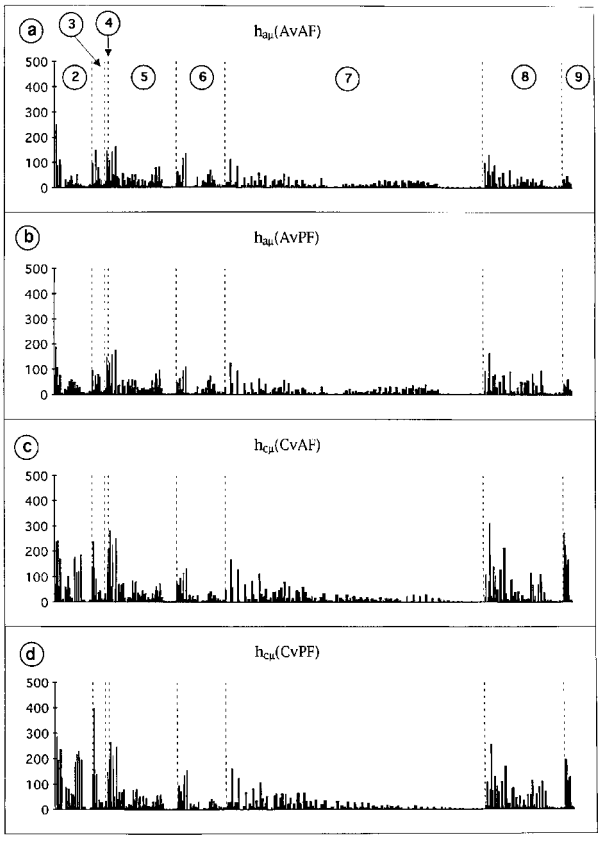

FIGURE 7. Frequency uncertainty test for molecules **2–9** of Figure 1 [HF / 6-31G(d, p) calculations]. (a) Uncertainties $h_{n\mu}$ for amplitudes AvAF in connection with adiabatic internal frequencies ω_a. (b) Uncertainties $h_{n\mu}$ for amplitudes AvPF in connection with adiabatic internal frequencies ω_a. (c) Uncertainties $h_{n\mu}$ for amplitudes CvAF in connection with **c**-vector frequencies ω_c. (d) Uncertainties $h_{n\mu}$ for amplitudes CvPF in connection with **c**-vector frequencies ω_c. In all cases, $h_{n\mu}$ points that correspond to $\Delta\mathscr{A} = 0$ for all tests in connection with a given molecule are removed.

PED performs satisfactory for the vibrational spectra of acyclic molecules with moderate coupling between internal modes. Comparative tests of the PED analysis as performed in this work were never done and, therefore, the deficiencies of the PED approach were never revealed.

THE CHOICE OF THE RIGHT METRIC

So far, different types of amplitudes ($A_{n\mu}$ or P^{μ}_{nn}) calculated with different vectors $\mathbf{v}_n$ (adiabatic or **c**-vectors) were tested. It remains to investigate the right choice of the metric **O** used in the definition of $\mathscr{A}$ [1]. In this connection, one can ask why the PED analysis for the characterization of normal modes was never formulated with the metric **O** = **S** = **I** rather than **O** = **f**, i.e., calculating amplitudes from the elements of the **D**-matrix according to

$$\mathscr{A}_{n\mu} = \frac{D^2_{n\mu}}{\sum_m D^2_{m\mu}}, \tag{3}$$

which is implicitly contained in the early work of Morino and Kuchitsu [8]. An answer to this question can be provided by using the frequency uncertainty test for AvAO-amplitudes and varying O. Different choices for O can be compared with the help of the differences

$$\begin{aligned}\Delta h_1 &= h(\text{AvAS}) - h(\text{AvAF})\\ \Delta h_2 &= h(\text{AvAS}) - h(\text{AvAM})\\ \Delta h_3 &= h(\text{AvAM}) - h(\text{AvAF}).\end{aligned} \tag{4}$$

In Figure 8, calculated differences Δh_1 [Fig. 8(a)], Δh_2 [Fig. 8(b)], and Δh_3 [Fig. 8(c)] are given for **1** (example with large coupling between internal modes) employing parameter sets PS1 (I in Fig. 8) and RPS5 (II in Fig. 8) and for molecules **2**–**9** (examples with moderate or relatively small coupling between internal modes). The corresponding averaged frequency uncertainties are listed in Table IV. Relative to either AvAM or AvAF amplitudes, AvAS amplitudes clearly lead to larger uncertainties, where differences Δh_1 and Δh_2 increase with increasing coupling between internal modes [Fig. 8(a) and (b)]. On the other hand, use of the metric **O** = **M** or **O** = **f** leads to about the same frequency uncertainties as is confirmed by $\Delta h_3 = h(\text{AvAM}) - h(\text{AvAF})$ shown in Figure 8(c). These results confirm that a PED analysis based on Eq. (5) and the metric **O** = **S** = **I** is inferior to the actual PED analysis with **O** = **f**. This was early realized by Morino and Kuchitsu in their basic article on the PED method [8].

Conclusions

According to the results obtained in this work, the method of characterizing normal vibrational modes (CNM) in terms of internal vibrational

TABLE III

Average frequency uncertainties for molecules 2–9 calculated at the HF / 6-31G(*d*, *p*) level of theory with the nonredundant PSs of Table I.

No.	Molecule	Sym	N_{vib}	AvAF	AvPF	CvAF	CvPF
Average frequency uncertainty: $\bar{h}_{n\mu}$							
2	Ethane	D_{3d}	18	10.8	14.2	21.9	24.1
3	Ethene	D_{2h}	12	20.7	21.9	31.7	32.4
4	Ethyne	$D_{\infty h}$	7	32.9	31.4	31.4	32.9
5	Benzene	D_{6h}	30	13.6	13.7	16.5	16.7
6	Cyclopropane	D_{3h}	21	12.8	13.0	13.7	13.4
7	Cyclohexane	D_{3d}	48	6.9	6.7	8.3	8.6
8	Propane	C_{2v}	27	9.0	9.9	15.1	16.9
9	Methane	T_d	9	13.1	13.1	46.7	46.3
Average frequency uncertainty per normal mode: $\bar{h}_{\mu}$							
2	Ethane	D_{3d}	18	194	256	394	434
3	Ethene	D_{2h}	12	248	263	380	389
4	Ethyne	$D_{\infty h}$	7	230	220	220	230
5	Benzene	D_{6h}	30	408	411	495	501
6	Cyclopropane	D_{3h}	21	269	273	288	281
7	Cyclohexane	D_{3d}	48	331	322	398	413
8	Propane	C_{2v}	27	243	267	408	456
9	Methane	T_d	9	118	118	420	417

modes is best carried out in the following way:

1. Adiabatic internal mode vectors rather than **c**-vectors are used since the former are clearly superior to the latter according to all tests carried out in this work (symmetry, PS stability, and frequency uncertainty test).
2. Internal mode and normal mode vectors are best compared with the help of the *A*-type amplitudes defined in article III [1]. *A*-type amplitudes are PS independent and lead to amplitude values in agreement with symmetry. According to the frequency uncertainty test, the appropriate metric for the scalar product $(\mathbf{l}_{\mu}, \mathbf{v}_n)$ is given by either the mass or the force constant matrix. Therefore, one can use either AvAM or AvAF amplitudes depending on whether one is interested more in the kinetic or dynamic aspects of molecular vibrations.

The three criteria worked out in this and the previous article [1], namely, symmetry, PS stability, and frequency uncertainty criteria, are perfectly suited to test the physical basis of any amplitude definition. Use of the various amplitudes reveals that the *P*-type amplitudes CvPF used in the PED analysis [8–10] are inappropriate for use in the CNM method. They combine the deficiencies of **c**-vectors with those of the **P**-matrix, which results in a large PS dependence and values difficult to explain. In view of our results, it is astonishing that the PED analysis has been used over three decades without searching for any alternatives.

It was also demonstrated that intrinsic frequencies, which can be based on **c**-vectors (or alternatively on **a**-vectors), can compensate some of their deficiencies by their construction as averaged frequencies. On the other hand, the frequency uncertainty test clearly reveals their overall poor performance in vibrational problems with relatively strong coupling between internal modes.

Both the PED analysis and its extension suggested by Boatz and Gordon [11] have been used without questioning their physical basis because their performance in the case of acyclic molecules or molecules with relatively small coupling between internal modes is satisfactory. There is also the possibility of improving PED results by adding more redundant internal parameters to the PS as was demonstrated in this work. However, this

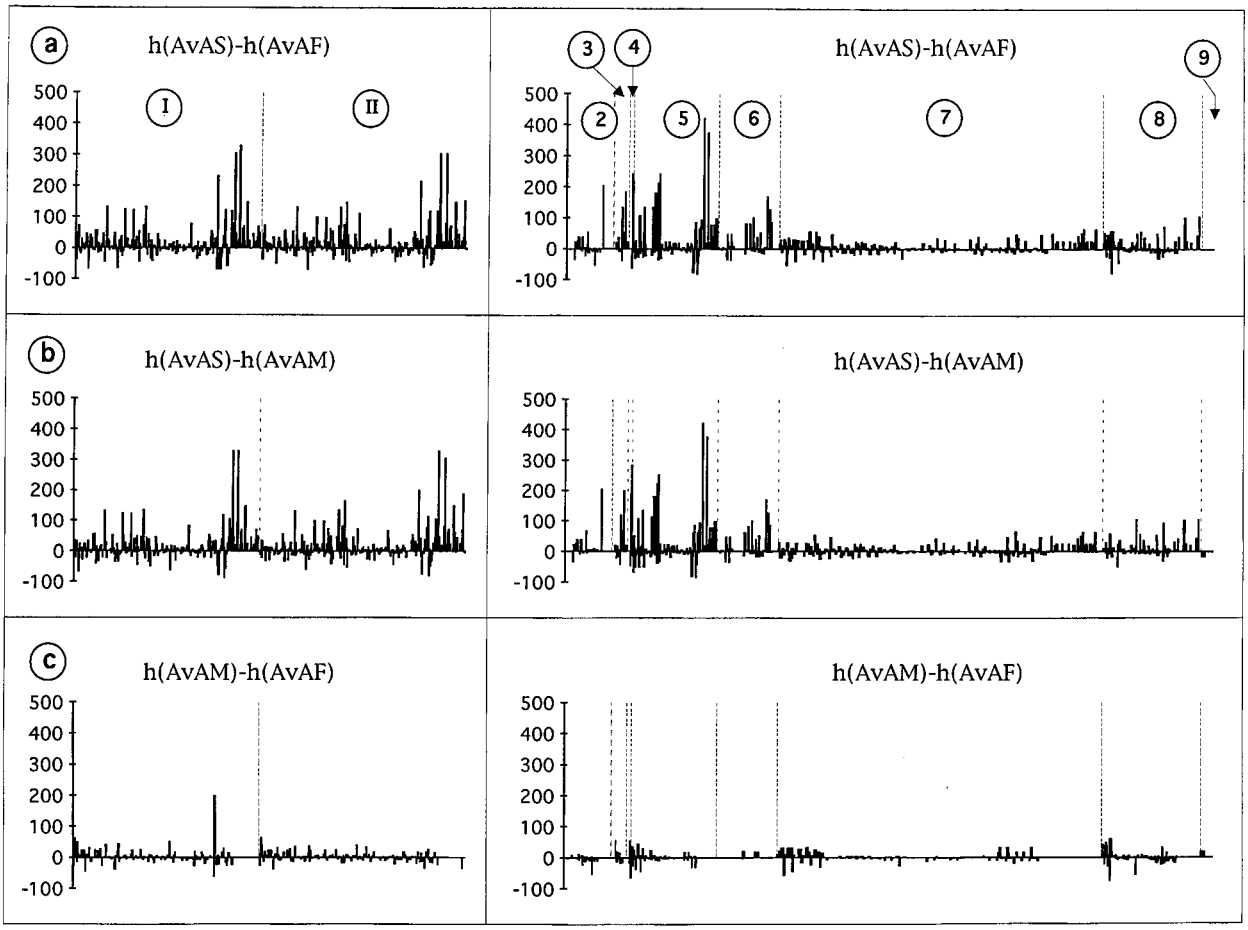

FIGURE 8. Frequency uncertainty test for molecules **1–9** of Figure 1 [HF / 6-31G(d, p) calculations]. Differences in uncertainties h(AvAO) in cm^{-1} obtained for metrics **O** = **S** = **I**, **M**, or **f** are given for parameters $\zeta_n = q_n$. (a) $\Delta h_1 = h(\text{AvAS}) - h(\text{AvAF})$; (b) $\Delta h_2 = h(\text{AvAS}) - h(\text{AvAM})$; (c) $\Delta h_3 = h(\text{AvAM}) - h(\text{AvAF})$. Points with $\mathscr{A}_{n\mu} = 0$ for all amplitude choices are removed.

TABLE IV

Average frequency uncertainties $\bar{h}_{n\mu}$ for molecules 1–9 calculated at the HF / 6-31G(d, p) level of theory for amplitudes AvAS, AvAM, and AvAF.

No.	Molecule	Sym	PS	AvAS	AvAM	AvAS−AvAF	AvAS−AvAM	AvAM−AvAF
1	Benzo-cyclobutadiene	C_{2v}	PS1	23.9	13.3	11.9	10.6	1.3
			RPS5	23.0	11.3	12.2	11.7	0.5
2	Ethane	D_{3d}	PS1	12.8	9.4	2.0	3.4	−1.4
3	Ethene	D_{2h}	PS1	37.5	22.4	16.8	15.1	1.7
4	Ethyne	$D_{\infty h}$	PS1	64.0	34.4	31.1	29.5	1.6
5	Benzene	D_{6h}	PS1	29.2	14.6	15.5	14.5	1.0
6	Cyclopropane	D_{3h}	PS1	20.3	13.6	7.4	6.7	0.7
7	Cyclohexane	D_{3d}	PS1	10.1	7.9	3.2	2.2	1.0
8	Propane	C_{2v}	PS1	13.6	9.9	4.6	3.7	0.8
9	Methane	T_d	PS1	13.1	14.5	−0.1	−1.4	1.3

approach is not generally applicable. In the case of an asymmetrical molecule, it is not possible to improve PED results in a systematic manner by changing the PS.

ACKNOWLEDGMENTS

This work was supported by the Swedish Natural Science Research Council (NFR). All calculations were done on the CRAY YMP/416 of the Nationellt Superdatorcentrum (NSC), Linköping, Sweden. The authors thank the NSC for a generous allotment of computer time.

References

1. Z. Konkoli and D. Cremer, Int. J. Quantum Chem. **67**, 29 (1998).
2. Z. Konkoli, J. A. Larsson, and D. Cremer, Int. J. Quantum. Chem. **67**, 1 (1998).
3. Z. Konkoli and D. Cremer, Int. J. Quantum. Chem. **67**, 11 (1998).
4. E. B. Wilson Jr., J. C. Decius, and P. C. Cross, *Molecular Vibrations, The Theory of Infrared and Raman Vibrational Spectra* (McGraw-Hill, London, 1955).
5. G. Herzberg, *Infrared and Raman Spectra of Polyatomic Molecules* (Van Nostrand, New York, 1945).
6. P. Gans, *Vibrating Molecules* (Chapman and Hall, London, 1971).
7. L. A. Woodward, *Introduction to the Theory of Molecular Vibrations and Vibrational Spectroscopy* (Clarendon Press, Oxford, 1972).
8. Y. Morino and K. Kuchitsu, J. Chem. Phys. **20**, 1809 (1952).
9. P. Pulay and F. Török, Acta Chim. Hung. **44**, 287 (1965).
10. G. Keresztury and G. Jalsovsky, J. Mol. Struct. **10**, 304 (1971).
11. J. A. Boatz and M. S. Gordon, J. Phys. Chem. **93**, 1819 (1989).
12. (a) N. Neto, Chem. Phys. **91**, 89, 101 (1984). (b) N. Neto, Chem. Phys. **87**, 43 (1984).
13. (a) D. Cremer and J. A. Pople, J. Am. Chem. Soc. **97**, 1354 (1975). (b) G. Fogarasi, X. Zhou, W.T. Patterson, and P. Pulay, J. Am. Chem. Soc. **114**, 8191 (1992).
14. P. C. Hariharan and J. A. Pople, Theor. Chim. Acta **28**, 213 (1973).